


Article

# Antioxidant and Cytoprotective Effects of Tibetan Tea and Its Phenolic Components

Hong Xie <sup>1,2,†</sup>, Xican Li <sup>1,2,\*,†</sup> , Zhenxing Ren <sup>3,4</sup>, Weimin Qiu <sup>1</sup>, Jianlan Chen <sup>1</sup>, Qian Jiang <sup>1,2</sup>, Ban Chen <sup>1,2</sup> and Dongfeng Chen <sup>3,4,\*</sup>

<sup>1</sup> School of Chinese Herbal Medicine, Guangzhou University of Chinese Medicine, Guangzhou 510006, China; xiehongxh1@163.com (H.X.); weiss99@163.com (W.Q.); 15219389939@163.com (J.C.); jiangqiande920711@163.com (Q.J.); 15119635373@163.com (B.C.)

<sup>2</sup> Innovative Research & Development Laboratory of TCM, Guangzhou University of Chinese Medicine, Guangzhou 510006, China; Guangzhou 510006, China

<sup>3</sup> School of Basic Medical Science, Guangzhou University of Chinese Medicine, Guangzhou 510006, China; 13192669534@163.com

<sup>4</sup> The Research Center of Basic Integrative Medicine, Guangzhou University of Chinese Medicine, Guangzhou 510006, China

\* Correspondence: lixican@126.com (X.L.); chen888@gzucm.edu.cn (D.C.); Tel.: +86-20-39358076

† These authors contributed equally to this work.

Received: 6 December 2017; Accepted: 23 January 2018; Published: 24 January 2018

**Abstract:** Tibetan tea (Kangzhuan) is an essential beverage of the Tibetan people. In this study, a lyophilized aqueous extract of Tibetan tea (LATT) was prepared and analyzed by HPLC. The results suggested that there were at least five phenolic components, including gallic acid, and four catechins (i.e., (+)-catechin, (–)-catechin gallate (CG), (–)-epicatechin gallate (ECG), and (–)-epigallocatechin gallate). Gallic acid, the four catechins, and LATT were then comparatively investigated by four antioxidant assays: ferric reducing antioxidant power, 2-phenyl-4,4,5,5-tetramethylimidazole-1-oxyl 3-oxide radical (PTIO•) scavenging, 1,1-diphenyl-2-picryl-hydrazyl radical scavenging, and 2,2'-azino-bis(3-ethylbenzo-thiazoline-6-sulfonic acid) radical scavenging assays. In these assays, LATT, along with the five phenolic components, increased their antioxidant effects in a concentration-dependent manner; however, the half maximal scavenging concentrations of ECG were always lower than those of CG. Gallic acid and the four catechins were also suggested to chelate Fe<sup>2+</sup> based on UV-visible spectral analysis. Ultra-performance liquid chromatography coupled with electrospray ionization quadrupole time-of-flight tandem mass spectrometry (UPLC–ESI–Q–TOF–MS/MS) analysis suggested that, when mixed with PTIO•, the five phenolic components could yield two types of radical adduct formation (RAF) products (i.e., tea phenolic dimers and tea phenolic-PTIO• adducts). In a flow cytometry assay, (+)-catechin and LATT was observed to have a cytoprotective effect towards oxidative-stressed bone marrow-derived mesenchymal stem cells. Based on this evidence, we concluded that LATT possesses antioxidative or cytoprotective properties. These effects may mainly be attributed to the presence of phenolic components, including gallic acid and the four catechins. These phenolic components may undergo electron transfer, H<sup>+</sup>-transfer, and Fe<sup>2+</sup>-chelating pathways to exhibit antioxidative or cytoprotective effects. In these effects, two diastereoisomeric CG and ECG showed differences to which a steric effect from the 2-carbon may contribute. Phenolic component decay may cause RAF in the antioxidant process.

**Keywords:** Kangzhuan; cytoprotection; catechins; steric effect; antioxidant mechanisms

## 1. Introduction

Tibetan tea (“Zangcha” in Chinese, Figure S1), a member of the fully fermented tea (dark tea) family, has a history of approximately 1000 years in China. It has become an essential beverage for millions of Tibetan people. The Tibetan Plateau varies in altitude between 3000 and 5000 meters and is not well-suited for cultivating vegetables, fruit, or trees. Thus, Tibetan people eat various meat products, such as beef, milk, and butter tea. These high-protein, high-lipid foods can effectively help them to resist the severe cold of high altitude. However, this diet may increase the risk of cardiovascular and indigestion diseases.

It has been reported that Tibetan tea can effectively lower blood pressure, remove blood lipids, and reduce the generation of atherosclerosis [1,2]. Intake of Tibetan tea is also hypothesized to blunt the effects of high-altitude hypoxia [3]. This tea is indispensable for Tibetan life and is thus called “Tibetan tea” by the Chinese, even though the tea is actually manufactured in Sichuan (a Han nationality Province in China). The tea is processed through five main working procedures with 30 processing technologies; these technologies were listed as Chinese Intangible Cultural Heritage in 2008 [4]. The whole process takes approximately 6 months, during which some chemical components have possibly degraded and some fungal populations have also been altered [5]. All of these give Tibetan tea a characteristic taste and potential beneficial effects.

Nevertheless, as a traditional tea with ethnological characteristics, Tibetan tea has received very little interest from scientists. In the PubMed database, only three papers about Tibetan tea can be retrieved from 1991 to 2016 [3,6,7].

According to their working procedures and materials, Tibetan tea products are classified into three main types: Kangzhuan, Jinjian, and Kangjian. The most popular type is Kangzhuan, i.e., brick tea. The present study attempted to use Kangzhuan as a representative to estimate the antioxidant or cytoprotective effects of Tibetan tea and examined the possible mechanisms.

## 2. Results and Discussion

In this study, the prepared LATT was analyzed by the HPLC method, and at least five phenolic components were found, including gallic acid (GA) and four catechins [(+)-catechin and its galloylated derivatives CG, ECG, and EGCG, Figure 1]. The contents of GA, (+)-catechin, EGCG, ECG, and CG were calculated as  $0.44 \pm 0.02$  g/100 g,  $0.11 \pm 0.01$  g/100 g,  $0.24 \pm 0.01$  g/100 g,  $0.13 \pm 0.01$  g/100 g, and  $0.04 \pm 0.01$  g/100 g, respectively. Each of their contents in LATT was lower than in green tea [8]. The difference was reported to be due to the comprehensive working protocols (especially fermentation [9]) and production seasons [10]. In the present study, their lower levels may also be related to the sample preparation. Our preliminary experiment using distilled water to dissolve LATT found the huge peaks of caffeine and gallic acid to severely interfere with the determination of other peaks. Thus, we had to use methanol to prepare LATT solution for determination. Methanol however cannot fully extract the phenolic components from a lyophilized aqueous extract. This also led to a lower level of caffeine ( $0.72 \pm 0.01$  g/100 g).

Our previous study demonstrated that the antioxidant capacity of plants can be mainly attributed to the existence of total phenolics [11]. In the present experiments, five phenolic components and LATT were comparatively evaluated using various antioxidant assays, including the ferric reducing antioxidant power (FRAP), PTIO•-scavenging, ABTS<sup>+</sup>•-scavenging, and DPPH•-scavenging assays. The half maximal scavenging concentration (SC<sub>50</sub>) values in these assays revealed that the five phenolic components always exhibited stronger antioxidant abilities than LATT itself (Table 1). On the basis of this evidence and previous reports [12,13], it can be assumed that these phenolic components may be responsible for the antioxidant effects of LATT. This is consistent with data from the flow cytometry assay, in which (+)-catechin (68.2%) gave a higher uninjured cell population than LATT (56.9%) (Figure 2). The study only measured (+)-catechin for cytoprotection because (+)-catechin possesses the basic, most typical skeleton (Figure 1), and other galloylated catechins (especially EGCG) have been widely studied for their cytoprotection previously [14–17].

As mentioned in the previous literature, the FRAP assay at pH 3.6 is essentially an electron-transfer (ET) process [18]. The data (Figure S2 and Table 1) showed that the five phenolic components in LATT could effectively increase the FRAP percentages, suggesting that these phenolic components may undergo the ET pathway to scavenge free radicals.

The ET pathway, however, is usually accompanied by an H<sup>+</sup>-transfer pathway [18]. The PTIO•-scavenging assay, an H<sup>+</sup>-transfer-involved reaction [19,20], was hence performed in the study. The five phenolic components and LATT dose-dependently increased their PTIO•-scavenging efficacies (Figure S3), indicating that H<sup>+</sup>-transfer may be involved in the antioxidant process.

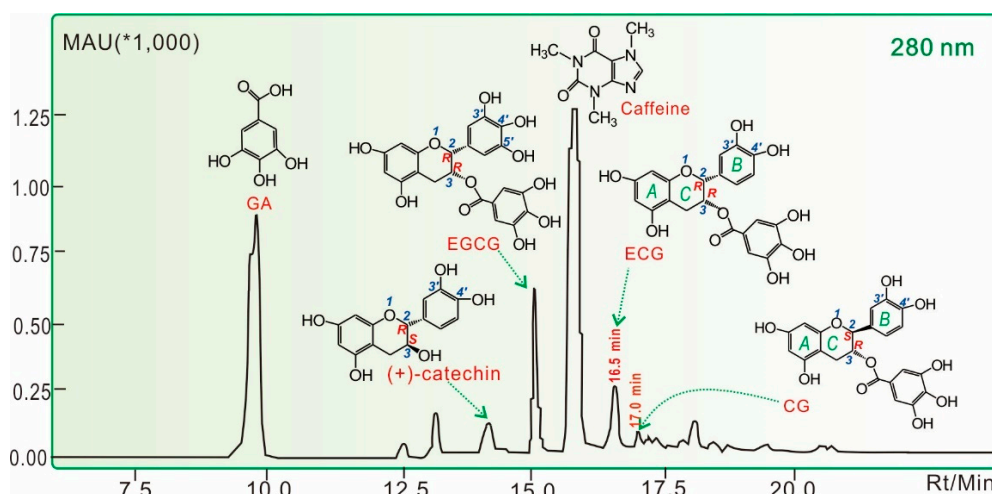


**Figure 1.** HPLC of LATT. GA, gallic acid; CG, (–)-catechin gallate; ECG, (–)-epicatechin gallate; EGCG, (–)-epigallocatechin gallate. The determining wavelength was 280 nm; The longitudinal axis was the strength of absorbance. MAU, milli-absorbance unit; Rt, retention time; Min, minute.

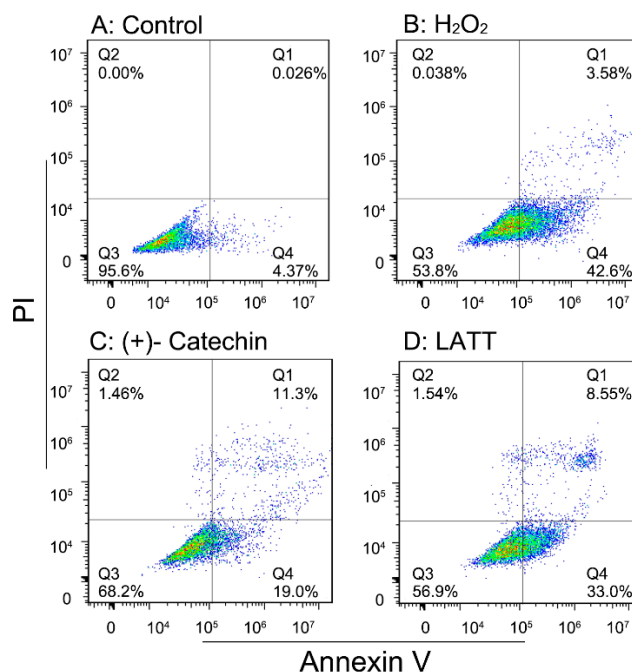


**Figure 2.** Typical flow cytometry diagram of cytoprotection of (+)-catechin and LATT in oxidatively stressed bmMSCs. The assay was conducted to distinguish live cells (Q3), necrotic cells (Q2), early apoptotic cells (Q4), and late apoptotic/necrotic cells (Q1).

**Table 1.** The FRAP and SC<sub>50</sub> values of LATT, ECG, EGCG, CG, C, GA, and Trolox.

	FRAP	PTIO●-Scavenging	ABTS <sup>+</sup> ●-Scavenging	DPPH●-Scavenging
LATT µg/mL	33.2 ± 1.2	531.9 ± 26.0	15.0 ± 0.4	48.7 ± 1.7
ECG µg/mL(µM)	2.7 ± 0.1 (6.0 ± 0.2 <sup>a</sup> )	23.1 ± 0.6 (52.2 ± 1.4 <sup>a</sup> )	0.8 ± 0.0 (1.8 ± 0.0 <sup>a</sup> )	2.5 ± 0.1 (5.7 ± 0.2 <sup>a</sup> )
EGCG µg/mL(µM)	4.9 ± 0.2 (10.9 ± 0.5 <sup>b</sup> )	23.8 ± 0.23 (53.7 ± 0.5 <sup>a</sup> )	1.4 ± 0.1 (3.0 ± 0.1 <sup>b</sup> )	2.9 ± 0.1 (6.9 ± 0.3 <sup>b</sup> )
CG µg/mL(µM)	5.3 ± 0.1 (11.9 ± 0.1 <sup>b</sup> )	28.2 ± 3.1 (63.8 ± 7.1 <sup>b</sup> )	1.3 ± 0.0 (2.9 ± 0.1 <sup>b</sup> )	4.1 ± 0.2 (9.4 ± 0.4 <sup>b</sup> )
(+)-catechin µg/mL(µM)	10.8 ± 0.5 (37.3 ± 1.9 <sup>d</sup> )	71.2 ± 4.0 (161.0 ± 9.1 <sup>d</sup> )	1.1 ± 0.0 (3.6 ± 0.1 <sup>c</sup> )	5.1 ± 0.1 (18.2 ± 0.3 <sup>d</sup> )
GA µg/mL(µM)	3.1 ± 0.1 (18.1 ± 0.8 <sup>c</sup> )	50.4 ± 0.64 (113.9 ± 1.4 <sup>c</sup> )	0.7 ± 0.0 (4.3 ± 0.2 <sup>d</sup> )	2.1 ± 0.1 (12.6 ± 0.4 <sup>c</sup> )
Trolox µg/mL(µM)	11.2 ± 0.2 (44.6 ± 1.0 <sup>e</sup> )	23.9 ± 0.7 (54.1 ± 1.5 <sup>a</sup> )	5.4 ± 1.2 (21.4 ± 4.9 <sup>f</sup> )	9.2 ± 1.1 (36.3 ± 4.5 <sup>e</sup> )

SC<sub>50</sub> values are expressed as the mean ± SD (*n* = 3). Mean values with different letters (a, b, c, d, e, or f) in same column are significantly different (*p* < 0.05). All dose–response curves are detailed in Figures 2–5.

It is worth mentioning that, after the ET and H<sup>+</sup>-transfer reaction, phenolic antioxidants may be transferred into free radicals. The phenolic antioxidant radical may form a covalent adduct with another free radical in the decay process. This is called a radical adduct formation (RAF) reaction [21]. As shown in Figure 3A,B, the reaction product of PTIO● with (+)-catechin gave a peak with *m/z* 579.2 at 1.03 min in the ultra-performance liquid chromatography coupled with electrospray ionization quadrupole time-of-flight tandem mass spectrometry (UPLC–ESI–Q–TOF–MS/MS) analysis. The *m/z* value (580) of the product was exactly double the molecular weight of (+)-catechin, and its secondary MS resembled (+)-catechin itself (Figure 3C), suggesting a dimerization reaction in the RAF pathway. In addition, (+)-catechin can react with PTIO● to give (+)-catechin-PTIO (*m/z* 520.9, Figure 3D–F).

As a galloylated derivative of (+)-catechin, EGCG was also found to yield a relevant EGCG-PTIO product (*m/z* 689.2, Figure 3G–I) and dimeric EGCG-EGCG (*m/z* 915.2, Figure 3J–K). In addition to EGCG, other galloylated derivatives (CG and ECG) similarly gave RAF products (Figures S6 and S7). GA also gave a dimer of GA-GA. The dimer was identified by a peak with *m/z* 339.0, which is exactly double the molecular weight of GA in primary MS spectra, which yielded secondary MS spectra similar to GA itself, i.e., *m/z* 125, 170 (Figure 3L–N and Figure S8). Taken together, GA and the four catechins could generate RAF products when mixing with PTIO● radicals. It can be deduced that GA and the four catechins undergo the RAF pathway to exert their antioxidant actions.

The above RAF results are generally consistent with previous findings from ABTS●<sup>+</sup>- and DPPH●-scavenging assays. ABTS●<sup>+</sup>- and DPPH●-scavenging actions have been shown to have multiple antioxidant pathways involved in hydrogen atom transfer (HAT) [22], ET [23,24], H<sup>+</sup>-transfer [25], sequential electron proton transfer [23,24,26], or RAF [27–29]. In the present study, the phenolic components in LATT effectively scavenged ABTS●<sup>+</sup> and DPPH● radicals (Table 1 and Figures S4 and S5). This further suggests that the phenolic components in LATT can undergo ET, H<sup>+</sup>-transfer, and RAF to display antioxidant (reactive oxygen species-scavenging) effects.

Reactive oxygen species generation is usually linked to transition metals (especially Fe<sup>2+</sup> and Cu<sup>+</sup>). For instance, Fe<sup>2+</sup> can catalyze H<sub>2</sub>O<sub>2</sub> to form ●OH radicals via the Fenton reaction (Fe<sup>2+</sup> + H<sub>2</sub>O<sub>2</sub> → Fe<sup>3+</sup> + ●OH + OH<sup>-</sup>) [26]. Thus, chelation of Fe<sup>2+</sup> in solution can greatly reduce the catalytic potential to inhibit ●OH generation [23,30]. In the present study, the five phenolic components and LATT exhibited Fe<sup>2+</sup>-chelating abilities. As shown in Figure 4A,B, GA bound Fe<sup>2+</sup> to generate a blue solution with λ<sub>max</sub> 583 nm absorption. The EGCG-Fe<sup>2+</sup> complex produced a dark-blue solution with λ<sub>max</sub> 594 nm. Each of the CG-Fe<sup>2+</sup> and ECG-Fe<sup>2+</sup> complexes gave a navy solution with λ<sub>max</sub> 585 nm. The (+)-catechin-Fe<sup>2+</sup> complex yielded a green solution with λ<sub>max</sub> = 462 nm. These data imply that all

five phenolic compounds and LATT exhibit Fe<sup>2+</sup>-chelating abilities and that Fe<sup>2+</sup>-chelation may play a role in the antioxidative process of LATT [31].

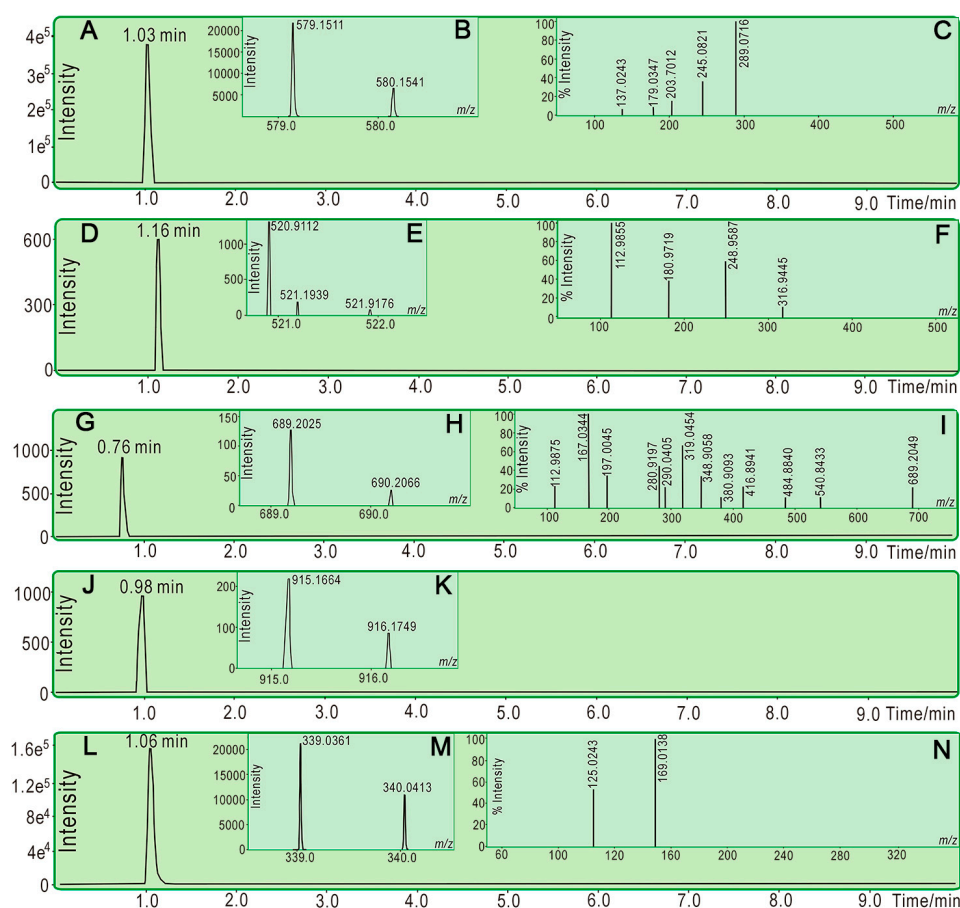


**Figure 3.** Typical UPLC–ESI–Q–TOF–MS/MS spectra of (+)-catechin (A–F) and (+)-catechin derivatives (G–K) for RAF investigation. (A) Chromatogram of RAF product of (+)-catechin-(+)-catechin when the formula  $[C_{30}H_{28}O_{12}-H]^-$  was extracted; (B) Primary MS spectra of RAF product of (+)-catechin-(+)-catechin; (C) secondary MS spectra of RAF product of (+)-catechin-(+)-catechin; (D) chromatogram of RAF product of C-PTIO when the formula  $[C_{28}H_{30}N_2O_8-H]^-$  was extracted; (E) primary MS spectra of RAF product of (+)-catechin-PTIO; (F) secondary MS spectra of RAF product of (+)-catechin-PTIO; (G) chromatogram of RAF product of EGCG-PTIO when the formula  $[C_{35}H_{34}N_2O_{13}-H]^-$  was extracted; (H) primary MS spectra of RAF product of EGCG-PTIO; (I) secondary MS spectra of RAF product of EGCG-PTIO.; (J) chromatogram of RAF product of EGCG-EGCG when the formula  $[C_{44}H_{36}O_{22}-H]^-$  was extracted; (K) primary MS spectra of RAF product of EGCG-EGCG. EGCG for the reference compound of (+)-catechin derivative; (L) chromatogram of RAF product of GA-GA when the formula  $[C_{14}H_{12}O_{10}-H]^-$  was extracted; (M) primary MS spectra of RAF product of GA-GA; (N) secondary MS spectra of RAF product of GA-GA. The other spectra are listed in 6–8.

It must be emphasized that CG and ECG are two diastereoisomers: CG and ECG take (2*S*, 3*R*) and (2*R*, 3*R*) absolute configurations, respectively. Thus, the sole difference between CG and ECG is the absolute steric configuration at the 2-carbon (Figures 1 and 6). This difference gives them distinctive molecular shapes. In the CG molecule, the B ring and galloyl moiety are arranged on two different sides, while they appear on the same side in ECG (Figure 5). Thus, an unbalanced array of chemical moieties enhances the polarity of ECG, and ECG (16.5 min) is eluted ahead of CG (17.0 min) in reversed-phase column HPLC (Figure 1). More importantly, such different steric configurations can

also affect antioxidant abilities, including radical-scavenging and  $\text{Fe}^{2+}$ -chelation. As shown in Table 1, ECG always exhibited higher antioxidant levels than CG in DPPH•-scavenging, ABTS<sup>+</sup>•-scavenging, PTIO•-scavenging, and FRAP assays. This may be because two very large ipsilateral moieties (*B* ring and galloyl moiety) may lead to repulsion to increase molecular energy and ET potential. This presumption is consistent with previous findings that *cis*-catechins exhibit a higher antioxidant ability than their epimers [32,33].

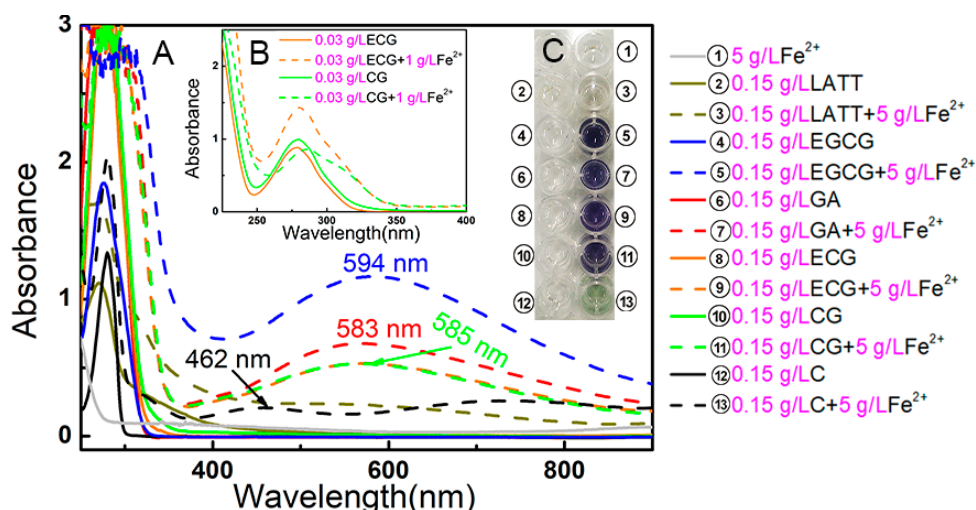


**Figure 4.** (A) UV spectra of  $\text{Fe}^{2+}$ -chelating complex; (B) UV-visible spectra of ECG and CG in  $\text{Fe}^{2+}$ -chelating reaction; (C) Appearance of solutions.

In  $\text{Fe}^{2+}$ -chelation, there is also a difference between CG and ECG. As illustrated in Figure 4B, ECG- $\text{Fe}^{2+}$  gave stronger UV absorbance than ECG itself, while CG- $\text{Fe}^{2+}$  exhibited weaker UV absorbance than CG itself. This difference can be explained by the absolute configurational difference at the 2-carbon. As two moieties with metal chelation potential [34,35], the *B* ring and the galloyl residue, are on the same side in ECG, this configuration can promote their synergistic binding to  $\text{Fe}^{2+}$ . This synergistic effect, however, cannot exist in CG, because they are separated distantly (Figure 5).

In a word, there are substantial differences between CG and ECG in terms of molecular polarity, radical scavenging, and  $\text{Fe}^{2+}$ -chelation. This stereochemistry may help us to further understand differences between catechins and corresponding “epi”-catechins [36,37].

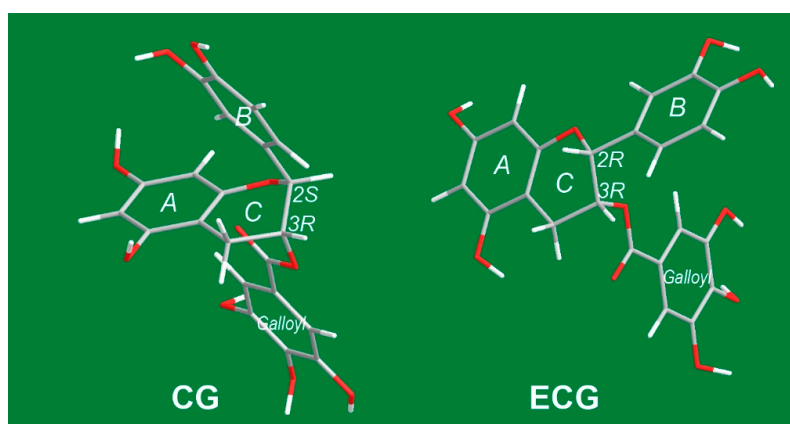


**Figure 5.** Stick-models of preferential conformations of CG and ECG (Red is for O atom; White is H and gray is C. Double bonds are not shown.).

### 3. Materials and Methods

#### 3.1. Animals and Chemicals

Tibetan tea (Kangzhuan, Lot No. 20120427) was purchased from Sichuan Ya'an Tea Factory Co., Ltd. (Sichuan, China). Sprague-Dawley (SD) rats (4 weeks) were obtained from the Animal Center of Guangzhou University of Chinese Medicine. (+)-Catechin ( $C_{15}H_{14}O_6$ , M.W. 290.27, CAS 154-23-4, 98%, Figure S9) was purchased from Shanghai Aladdin Chemistry Co., Ltd. (Shanghai, China). (–)-Epicatechin gallate (ECG,  $C_{22}H_{18}O_{10}$ , M.W. 442.37, CAS 1257-08-5, 98%, Figure S9) and (–)-epigallocatechin gallate (EGCG,  $C_{22}H_{18}O_{11}$ , M.W. 458.37, CAS 989-51-5, 98%, Figure S9) were purchased from Sichuan Weikeqi Biological Technology Co., Ltd. (Chengdu, China). (–)-Catechin gallate (CG,  $C_{22}H_{18}O_{10}$ , M.W. 442.37, CAS 130405-40-2, 98%, Figure S9) and gallic acid (GA,  $C_7H_6O_5$ , M.W. 170.12, CAS 149-91-7, 98%, Figure S9) were obtained from Chengdu PureChem-Standard Co., Ltd. (Chengdu, China). Caffeine (CAS 58-08-2, 98%) was from the Guangdong Guanghua Chemical Factory Co., Ltd. (Shantou, China). DPPH• (1,1-diphenyl-2-picryl-hydrazyl radical), Trolox ( $\pm$  -6-hydroxyl-2,5,7,8-tetramethylchromane-2-carboxylic acid), and 2,4,6-tripyridyl triazine (TPTZ) were purchased from Sigma-Aldrich Shanghai Trading Co. (Shanghai, China). PTIO• (2-phenyl-4,4,5,5-tetramethylimidazoline-1-oxyl-3-oxide radical) was from TCI Chemical Co. (Shanghai, China).  $(NH_4)_2ABTS$  [2,2'-azino-bis(3-ethylbenzo-thiazoline-6-sulfonic acid) diammonium salt] was obtained from the Amresco Chemical Co. (Solon, OH, USA). Low-glucose Dulbecco's modified Eagle's medium (L-DMEM), fetal bovine serum (FBS), and trypsin were purchased from Gibco (Grand Island, NY, USA). An annexin V/propidium iodide (PI) assay kit was purchased from Abcam (Cambridge, UK). Methanol and water were of HPLC grade. All other reagents used in this study were purchased as analytical grade from the Guangzhou Chemical Reagent Factory (Guangzhou, China).

#### 3.2. Preparation of Lyophilized Aqueous Extract of Tibetan Tea (LATT)

Tibetan tea was extracted based on the guidance of the manufacturer. In brief, the newly-purchased Tibetan tea (Kangzhuan) was decocted twice using 50-fold distilled water at 100 °C for 5 min. The extract was concentrated and lyophilized to prepare a lyophilized aqueous extract of Tibetan tea (LATT, Figure S10 and Figure 6). LATT was stored at 4 °C for further exploration.

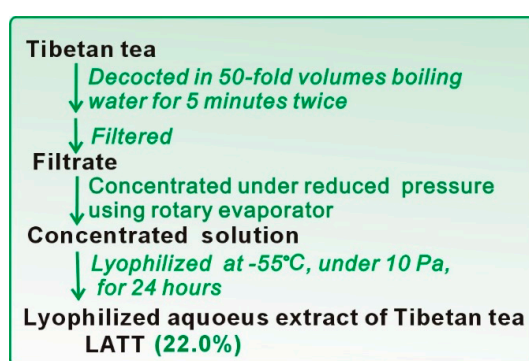


Figure 6. Preparation of LATT.

#### 3.3. HPLC Analysis for Phenolic Components in LATT

The LATT methanolic solution (48.6 mg/mL) was analyzed using an HPLC method. The HPLC analysis was performed on a Shimadzu LC-20A (Shimadzu Co., Kyoto, Japan) equipped with an Agilent 5 TC-C<sub>18</sub> (250 mm × 4.6 mm, 5 μm) (Agilent Technologies Inc., Palo Alto, CA, USA). The mobile phase consisted of A (methanol) and B (0.5% formic acid in water) with gradient elution: 0–5 min (90–70% B), 5–9 min (70–50% B), 9–13 min (50–40% B), 13–20 min (maintain 40% B), 20–22 min

(40–90% B), and 22–25 min (remain 90% B). The flow rate was 0.8 mL/min, injection volume was 20  $\mu$ L, column temperature was 35  $^{\circ}$ C, and absorption was measured at 280 nm. In the study, GA, (+)-catechin, EGCG, ECG, CG, and caffeine were identified by comparing their retention times with those of authentic samples.

#### 3.4. Ferric Reducing Antioxidant Power (FRAP) Assay

The FRAP assay was carried out based on Benzie and Strain's method [36]. Briefly, the FRAP reagent was prepared freshly by mixing 10 mM TPTZ, 20 mM FeCl<sub>3</sub>, and 0.25 M acetate buffer (pH 3.6) at 1:1:10. The test sample ( $x = 2$ –10  $\mu$ L) was added to  $(20 - x)$   $\mu$ L of 95% ethanol followed by 80  $\mu$ L of FRAP reagent. After incubation for 30 min, the mixture was measured for the  $A_{593\text{nm}}$  value at ambient temperature using distilled water as the blank. The relative reducing antioxidant power of the sample compared to the maximum absorbance was calculated by the following formula:

$$\text{Relative reducing effect \%} = \frac{A - A_{\min}}{A_{\max} - A_{\min}} \times 100\%$$

where  $A_{\min}$  is the lowest  $A_{593\text{nm}}$  value in the experiment,  $A$  is the  $A_{593\text{nm}}$  value of the reaction mixture with sample, and  $A_{\max}$  is the greatest  $A_{593\text{nm}}$  value in the experiment.

#### 3.5. Free Radical-Scavenging Assays In Vitro

The free radical-scavenging assays included the PTIO $\bullet$ -scavenging assay, DPPH $\bullet$ -scavenging assay, and ABTS $^{+\bullet}$ -scavenging assay. The PTIO $\bullet$ -scavenging assay was based on our method [22]. In brief, 80  $\mu$ L of aqueous PTIO $\bullet$  solution (0.1 mM) was mixed with 20  $\mu$ L of an aqueous or alcoholic solution of sample at various concentrations. The mixture was incubated at 50  $^{\circ}$ C for 30 min, and the absorbance at 560 nm was measured using a microplate reader (Multiskan FC, Thermo Scientific, Shanghai, China). The PTIO $\bullet$ -scavenging capacity % was calculated as:

$$\text{Scavenging capacity \%} = \frac{A_0 - A}{A_0} \times 100\%$$

where  $A_0$  is the absorbance of the control without sample and  $A$  is the absorbance of the reaction mixture with sample.

The ABTS $^{+\bullet}$ -scavenging assay was based on a previous report [37]. ABTS $^{+\bullet}$  was produced by mixing 200  $\mu$ L of (NH<sub>4</sub>)<sub>2</sub>ABTS (7.4 mM) with 200  $\mu$ L of K<sub>2</sub>S<sub>2</sub>O<sub>8</sub> (2.6 mM). After incubation in the dark for 12 h, the mixture was diluted with methanol (approximately 1:20) so that the absorbance at 734 nm was  $0.30 \pm 0.01$ . Then, the diluted ABTS $^{+\bullet}$  solution (80  $\mu$ L) was added to 20  $\mu$ L of an ethanolic (or aqueous) solution of sample at various concentrations and mixed thoroughly. After the reaction mixture stood for 3 min, the absorbance at 734 nm was measured using a microplate reader. The ABTS $^{+\bullet}$ -scavenging capacity % was calculated using the formula described in the PTIO $\bullet$ -scavenging assay.

The DPPH $\bullet$ -scavenging assay was based on previous reports [38]. In the assay, 80  $\mu$ L of an ethanolic solution of DPPH $\bullet$  (0.1 mM) was mixed with 20  $\mu$ L of an ethanolic (or aqueous) solution of sample at various concentrations. After incubation for 30 min, the mixture was measured for absorbance at 519 nm. The DPPH $\bullet$ -scavenging capacity % was calculated using the formula described in the PTIO $\bullet$ -scavenging assay. SC<sub>50</sub> was defined as the antioxidant concentration to give a scavenging capacity % half the value of that in the absence of antioxidant.

#### 3.6. UPLC–ESI–Q–TOF–MS/MS Analysis of Reaction Products of PTIO $\bullet$ with Phenolic Components

UPLC–ESI–Q–TOF–MS/MS spectra of reaction products of PTIO $\bullet$  with phenolic components were determined according to the method described by our report [39]. The methanolic solutions of phenolic components were mixed with a solution of PTIO $\bullet$  radicals in methanol at a molar ratio of 1:2,



and the resulting mixtures were incubated for 24 h at room temperature. The product mixtures were filtered through a 0.22- $\mu\text{m}$  filter and measured using a UPLC-ESI-Q-TOF-MS/MS system equipped with a  $\text{C}_{18}$  column (2.0 mm i.d.  $\times$  100 mm, 2.2  $\mu\text{m}$ , Shimadzu Co., Kyoto, Japan). The mobile phase was used for elution and consisted of a mixture of methanol (phase A) and water (phase B). The column was eluted at a flow rate of 0.3 mL/min with the following gradient elution program: 0–10 min, 60–100% A; 10–15 min, 100% A. The sample injection volume was set at 1  $\mu\text{L}$  to separate the components, column temperature was 40  $^{\circ}\text{C}$ ; Q-TOF-MS/MS analysis was conducted with a Triple TOF 5600 *plus* mass spectrometer (AB SCIEX, Framingham, MA, USA) equipped with an ESI source, which was run in the negative ionization mode. The scan range was set at 100–2000 Da. The system was run with the following parameters: ion spray voltage,  $-4500\text{ V}$ ; ion source heater, 550  $^{\circ}\text{C}$ ; curtain gas (CUR,  $\text{N}_2$ ), 30 psi; nebulizing gas (GS1, air), 50 psi; Tis gas (GS2, air), 50 psi. The declustering potential (DP) was set at  $-100\text{ V}$ , whereas the collision energy (CE) was set at  $-40\text{ V}$  with a collision energy spread (CES) of 20 V. The RAF products were quantified by extracting the corresponding formula (e.g.,  $[\text{C}_{28}\text{H}_{30}\text{N}_2\text{O}_8\text{-H}]^-$  for (+)-catechin-PTIO• and  $[\text{C}_{30}\text{H}_{28}\text{O}_{12}\text{-H}]^-$  for (+)-catechin dimer) from the total ion chromatogram and integrating the corresponding peak.

### 3.7. Cytoprotective Effect Assay

The MSC culture was performed in terms of our previous reports with slight modifications [14,40]. Briefly, bone marrow was obtained from the femur and tibia of rats. The marrow samples were diluted with L-DMEM containing 10% FBS. MSCs were prepared by gradient centrifugation at  $900\times g$  for 30 min on 1.073 g/mL Percoll. The prepared cells were transferred into culture flasks at a density of  $1\times 10^4/\text{cm}^2$ . The MSCs at passage 3 were estimated for cultured cell homogeneity using detection of CD44 by flow cytometry and used for the investigation. Injured MSCs were prepared by treatment with  $\text{H}_2\text{O}_2$  (200  $\mu\text{M}$ ). After incubation for 3 h, MSCs in the control group and  $\text{H}_2\text{O}_2$  group were incubated for 24 h in DMEM, while MSCs in the sample groups were incubated for 24 h in DMEM with (+)-catechin and LATT.

After culturing, cells were assayed using flow cytometry [41]. Briefly, the cultured cells were harvested with trypsin (0.05%) digestion in phosphate-buffered saline (PBS). The cells ( $5\times 10^5$ ) were collected by centrifugation and then resuspended in 500  $\mu\text{L}$  of binding buffer. At the same time, 5  $\mu\text{L}$  of annexin V-FITC and 5  $\mu\text{L}$  of propidium iodide were added. After incubation at room temperature for 5 min in the dark, fluorescence was measured by flow cytometry (Accuri C6, Franklin Lakes, BD, USA) with standard software.

### 3.8. UV Spectral Determination of $\text{Fe}^{2+}$ -Chelation

UV spectra for the  $\text{Fe}^{2+}$ -chelation of LATT and its phenolic components were determined according to the method described by our report [42–44]. Briefly, 75  $\mu\text{L}$  of a methanolic solution of sample (1 mg/mL) and 25  $\mu\text{L}$  of an aqueous solution of  $\text{FeCl}_2\cdot 4\text{H}_2\text{O}$  (100 mg/mL) were added to 400  $\mu\text{L}$  of an aqueous mixture of distilled water and methanol (1:1). The solution was mixed vigorously. The resulting mixture was incubated at room temperature for 1 h. Subsequently, the product mixture was collected and a spectrum was obtained using a UV-visible spectrophotometer (Unico UV 2600A, Unico Co., Shanghai, China) from 200 to 900 nm. Next, 200  $\mu\text{L}$  of the supernatant was transferred to a 96-well plate and photographed using a smartphone.

### 3.9. Statistical Analysis

The  $\text{SC}_{50}$  values were obtained by linear regression analysis. All linear regression analysis was conducted with Origin 6.0 professional software. Measurement of significant differences between the mean  $\text{SC}_{50}$  values of the sample and positive controls was performed using one-way ANOVA or the T-test. The analysis was performed using SPSS software 13.0 (SPSS Inc., Chicago, IL, USA) for Windows.  $p < 0.05$  was considered to be significant.

#### 4. Conclusions

Tibetan tea comprises at least five phenolic components, i.e., GA and four catechins [(+)-catechin, CG, ECG, and EGCG]. The antioxidant or cytoprotective effects of LATT may mainly be attributed to the existence of GA, four catechins, and other phenolic components. Among the four catechins, (+)-catechin was demonstrated to protect bmMSCs from oxidative stress-induced apoptosis. GA and the four catechins may undergo ET, H<sup>+</sup>-transfer, and Fe<sup>2+</sup>-chelating pathways to exhibit antioxidative or cytoprotective effects. In these effects, diastereoisomeric CG and ECG were different, and the difference can be attributed to that of a steric effect at the 2-carbon. Phenolic component decay may give rise to RAF products in the antioxidant process.

**Supplementary Materials:** The following are available online. Figure S1: The photo of Tibetan tea. Figure S2: (A) The dose–response curves of catechins and positive controls from FRAP assay. (B) The dose–response curves of LATT from FRAP assay. Figure S3: (A) The dose–response curves of catechins and Trolox in PTIO• scavenging. (B) The dose–response curves of LATT in PTIO• scavenging. Figure S4: (A) The dose–response curves of catechins and positive controls in ABTS<sup>+</sup>•-scavenging. (B) The dose–response curves of LATT in ABTS<sup>+</sup>•-scavenging. Figure S5: (A) The dose–response curves of catechins and positive controls in DPPH•-scavenging. (B) The dose–response curves of LATT in DPPH•-scavenging. Figure S6: (A) Chromatogram of RAF product of (–)-epigallocatechin gallate-(–)-epigallocatechin gallate when formula [C<sub>44</sub>H<sub>36</sub>O<sub>20</sub>-H]<sup>–</sup> was extracted. (B) Primary MS spectra of RAF product of (–)-epigallocatechin gallate-(–)-epigallocatechin gallate. (C) Secondary MS spectra of RAF product of (–)-epigallocatechin gallate-(–)-epigallocatechin gallate. Figure S7: (A) Chromatogram of RAF product of (–)-catechin gallate-(–)-catechin gallate when formula [C<sub>44</sub>H<sub>36</sub>O<sub>20</sub>-H]<sup>–</sup> was extracted. (B) Primary MS spectra of RAF product of (–)-catechin gallate-(–)-catechin gallate. (C) Secondary MS spectra of RAF product of (–)-catechin gallate-(–)-catechin gallate. Figure S8: Secondary MS spectra of gallic acid. Figure S9: Certificates of analysis of gallic acid, (+)-catechin, (–)-catechin gallate (CG), (–)-epicatechin gallate (ECG), and (–)-epigallocatechin gallate (EGCG). Figure S10: The appearance of the lyophilized aqueous extract of Tibetan tea.

**Acknowledgments:** This work was supported by the Guangdong Science and Technology Project (2017A030312009, 2017A050506043) and the National Nature Science Foundation of China (81573558).

**Author Contributions:** Xican Li and Dongfeng Chen conceived and designed the experiments; Hong Xie performed the chemical experiments; Zhenxing Ren performed the flow cytometry; Weimin Qiu, Hong Xie, and Jianlan Chen performed the antioxidant experiments; Qian Jiang analyzed the data; Xican Li wrote the paper; Ban Chen drew the diagrams. All authors read and approved the final manuscript.

**Conflicts of Interest:** The authors declare that they have no competing interests.

#### Abbreviations

The following abbreviations are used in this manuscript:

ABTS	[2,2′-azino-bis(3-ethylbenzo-thiazoline-6-sulfonic acid diammonium salt)]
bmMSCs	bone marrow-derived mesenchymal stem cells
CG	(–)-catechin gallate
DMEM	Dulbecco’s modified Eagle’s medium
DPPH•	1,1-diphenyl-2-picryl-hydrazyl
ET	electron transfer
ECG	(–)-epicatechin gallate
EGCG	(–)-epigallocatechin gallate
FBS	fetal bovine serum
FRAP	ferric reducing antioxidant power
GA	gallic acid
HAT	hydrogen atom transfer
LATT	lyophilized aqueous extract of <i>Tibetan tea</i>
PTIO•	2-phenyl-4,4,5,5-tetramethylimidazole-1-oxyl 3-oxide radical
ROS	reactive oxygen species
RAF	radical adduct formation
SD	standard deviation
TPTZ	2,4,6-tris(2-pyridyl-s-triazine)

## References

1. Jiang, A.L.; He, Y.B.; Hu, W.Z.; Liu, C.H.; Xu, G.K. The inheritance and development of Ya'an Tibetan tea. *Sci. Technol. Food Ind.* **2012**, *33*, 391–394.
2. Lu, X.H.; Xu, J.Y.; Sun, R.; Wang, J.Y. Human trial of health effects of Tibetan tea. *Food Res. Dev.* **2017**, *38*, 168–171.
3. Larrick, J.W. The methyl xanthine hypothesis: Does tea consumption by Tibetan natives blunt the effects of high altitude? *Med. Hypotheses* **1991**, *34*, 99–104. [[CrossRef](#)]
4. Lai, X. Ya'an Tibetan tea: The treasures of Chinese intangible cultural heritage. *Sichuan Provincial Cond.* **2012**, *4*, 33–35.
5. Zhong, T.; Qi, G.N.; Xu, W.; Chen, S.X.; Li, J.H. Identification of fungal populations during the storage period of Tibetan tea. *Guizhou Agri. Sci.* **2010**, *38*, 101–103.
6. Wu, J.; Wang, W.; Liu, Y.; Sun, J.; Ye, Y.; Li, B.; Liu, X.; Liu, H.; Sun, Z.; Li, M.; et al. Modifying role of GSTP1 polymorphism on the association between tea fluoride exposure and the brick-tea type fluorosis. *PLoS ONE* **2015**, *10*, e128280. [[CrossRef](#)] [[PubMed](#)]
7. Cao, J.; Bai, X.; Zhao, Y.; Liu, J.; Zhou, D.; Fang, S.; Jia, M.; Wu, J. The relationship of fluorosis and brick tea in Chinese Tibetan people. *Environ. Health Perspect.* **1996**, *104*, 1340–1343. [[CrossRef](#)] [[PubMed](#)]
8. Bae, I.K.; Ham, H.M.; Jeong, M.H.; Kim, D.H.; Kim, H.J. Simultaneous determination of 15 phenolic compounds and caffeine in teas and mate using RP-HPLC/UV detection: Method development and optimization of extraction process. *Food Chem.* **2015**, *172*, 469–475. [[CrossRef](#)] [[PubMed](#)]
9. Marini, F.; Beer, D.; Walters, N.A.; Villiers, A.; Joubert, E.; Walczak, B. Multivariate analysis of variance of designed chromatographic data. A case study involving fermentation of rooibos tea. *J. Chromatogr. A* **2017**, *1489*, 115–125. [[CrossRef](#)] [[PubMed](#)]
10. Joubert, E.; Beelders, T.; Beer, D.; Malherbe, C.J.; Villiers, A.J.; Sigge, G.O. Variation in phenolic content and antioxidant activity of fermented rooibos herbal tea infusions: role of production season and quality grade. *J. Agric. Food Chem.* **2012**, *60*, 9171–9179. [[CrossRef](#)] [[PubMed](#)]
11. Li, X.C.; Chen, D.F.; Mai, Y.; Wen, B.; Wang, X.Z. Concordance between antioxidant activities in vitro and chemical components of Radix Astragali. *Nat. Prod. Res.* **2012**, *26*, 1050–1053. [[CrossRef](#)] [[PubMed](#)]
12. Li, X.C.; Jiang, Q.; Wang, T.; Liu, J.; Chen, D. Comparison of the antioxidant effects of quercitrin and isoquercitrin: Understanding the role of the 6''-OH group. *Molecules* **2016**, *21*, 1246. [[CrossRef](#)] [[PubMed](#)]
13. Rusak, G.; Komes, D.; Likic, S.; Horzic, D.; Kovac, M. Phenolic content and antioxidative capacity of green and white tea extracts depending on extraction conditions and the solvent used. *Food Chem.* **2008**, *110*, 852–858. [[CrossRef](#)] [[PubMed](#)]
14. Chen, D.F.; Li, X.C.; Xu, Z.; Liu, X.; Du, S.H.; Li, H.; Zhou, J.H.; Zeng, H.P.; Hua, Z.C. Hexadecanoic acid from Buzhong Yiqi decoction induces proliferation of bone marrow mesenchymal stem cells. *J. Med. Food.* **2010**, *13*, 967–970. [[CrossRef](#)] [[PubMed](#)]
15. Li, X.C.; Wei, G.; Wang, X.Z.; Liu, D.H.; Deng, R.D.; Li, H.; Zhou, J.H.; Li, Y.W.; Zeng, H.P.; Chen, D.F. Targeting of the sonic hedgehog pathway by atractylenolides promotes chondrogenic differentiation of mesenchymal stem cells. *Biol. Pharm. Bull.* **2012**, *35*, 1328–1335. [[CrossRef](#)] [[PubMed](#)]
16. Du, G.J.; Zhang, Z.Y.; Wen, X.D.; Yu, C.H.; Calway, T.; Yuan, C.S.; Wang, C.Z. Epigallocatechin Gallate (EGCG) is the most effective cancer chemopreventive polyphenol in green tea. *Nutrients* **2012**, *4*, 1679–1691. [[CrossRef](#)] [[PubMed](#)]
17. Kim, H.S.; Quon, M.J.; Kim, J.A. New insights into the mechanisms of tea-phenolics beyond antioxidant properties; lessons from the green tea polyphenol, epigallocatechin-3-gallate. *Redox Biol.* **2014**, *2*, 187–195. [[CrossRef](#)] [[PubMed](#)]
18. Gülçin, İ. Antioxidant activity of food constituents: an overview. *Arch. Toxicol.* **2012**, *86*, 345–391. [[CrossRef](#)] [[PubMed](#)]
19. Mayer, J.M.; Rhile, I.J.; Larsen, F.B.; Mader, E.A.; Markle, T.F.; DiPasquale, A.G. Models for proton-coupled electron transfer in Photosystem II. *Photosynth. Res.* **2006**, *87*, 3–20. [[CrossRef](#)] [[PubMed](#)]
20. Goldstein, S.; Russo, A.; Samuni, A. Reactions of PTIO• and carboxy-PTIO• with •NO, •NO<sub>2</sub>, and O<sub>2</sub>. *J. Biol. Chem.* **2003**, *278*, 50949–50955. [[CrossRef](#)] [[PubMed](#)]
21. Li, X.; Wang, T.; Liu, J.; Liu, Y.; Zhang, J.; Lin, J.; Zhao, Z.; Chen, D. Effect and mechanism of wedelolactone as antioxidant-coumestan on •OH-treated mesenchymal stem cells. *Arab J. Chem.* **2017**. [[CrossRef](#)]

22. Li, X.C. 2-phenyl-4,4,5,5-tetramethylimidazoline-1-oxyl 3-oxide (PTIO●) radical-scavenging: a new and simple antioxidant assay in vitro. *J. Agric. Food Chem.* **2017**, *65*, 6288–6297. [[CrossRef](#)] [[PubMed](#)]
23. Li, X.C.; Han, W.; Mai, W.; Wang, L. Antioxidant Activity and mechanism of tetrahydroamentoflavone in vitro. *Nat. Prod. Commun.* **2013**, *8*, 787–789.
24. Lin, J.; Li, X.C.; Chen, L.; Chen, D.F. Protective effect against hydroxylradical-induced DNA damage and antioxidant mechanism of [6]-gingerol: A chemical study. *Bull Korean Chem. Soc.* **2014**, *35*, 1633–1638. [[CrossRef](#)]
25. Musialik, M.; Litwinienko, G. Scavenging of DPPH● radicals by Vitamin E is accelerated by its partial ionization: the role of sequential proton loss electron transfer. *Org. Lett.* **2005**, *7*, 4951–4954. [[CrossRef](#)] [[PubMed](#)]
26. Li, X.C.; Hu, Q.P.; Jiang, S.X.; Li, F.; Lin, J.; Han, L.; Hong, Y.L.; Lu, W.B.; Gao, Y.X.; Chen, D.F. Flos *chrysanthemi indicis* protects against hydroxyl-induced damages to DNA and MSCs via antioxidant mechanism. *J. Saudi Chem. Soc.* **2015**, *19*, 454–460. [[CrossRef](#)]
27. Osman, A.M.; Wong, K.K.Y.; Fernyhough, A. ABTS radical-driven oxidation of polyphenols: Isolation and structural elucidation of covalent adducts. *Biochem. Biophys. Res. Commun.* **2006**, *346*, 321–329. [[CrossRef](#)] [[PubMed](#)]
28. Lópezmartínez, L. M.; Santacruzortega, H.; Navarro, R. E.; Sotelomundo, R.R.; Gonzálezaguilar, G.A. A <sup>1</sup>H-NMR investigation of the interaction between phenolic acids found in mango (*manguifera indica* cv ataulfo) and papaya (*carica papaya* cv maradol) and 1,1-diphenyl-2-picrylhydrazyl (dpph) free radicals. *PLoS ONE* **2015**, *10*, e0140242.
29. Osman, A.M. Multiple pathways of the reaction of 2,2-diphenyl-1-picrylhydrazyl radical (DPPH) with (+)-catechin: Evidence for the formation of a covalent adduct between DPPH and the oxidized form of the polyphenol. *Biochem. Biophys. Res. Commun.* **2011**, *412*, 473–478. [[CrossRef](#)] [[PubMed](#)]
30. Perron, N.R.; Brumaghim, J.L. A review of the antioxidant mechanisms of polyphenol compounds related to iron chelating. *Cell Biochem. Biophys.* **2009**, *53*, 75–100. [[CrossRef](#)] [[PubMed](#)]
31. Fang, Y.Z.; Zheng, R.L. *Theory and Application of Free Radical Biology*; Science Press: Beijing, China, 2002; pp. 56–78.
32. Tu, Y.; Yang, X.; Kong, J.; Zhang, S.; Zhu, Y.; Wang, Y. Antioxidant capability of Epi-catechins and theaflavins in vitro by scavenging hydroxyl free radical. *Nat. Prod. Res. Dev.* **2012**, *24*, 653–659.
33. Lee, L.S.; Kim, S.H.; Kim, Y.B.; Kim, Y.C. Quantitative analysis of major constituents in green tea with different plucking periods and their antioxidant activity. *Molecules* **2014**, *19*, 9173–9186. [[CrossRef](#)] [[PubMed](#)]
34. Li, X.C.; Liu, J.; Lin, J.; Wang, T.; Huang, J.; Lin, Y.; Chen, D. Protective effects of dihydromyricetin against ●OH-induced mesenchymal stem cells damage and mechanistic chemistry. *Molecules* **2016**, *21*, 604. [[CrossRef](#)] [[PubMed](#)]
35. Liu, J.J.; Li, X.C.; Lin, J.; Li, Y.R.; Wang, T.T.; Jiang, Q.; Chen, D.F. *Sarcandra glabra* (Caoshanhu) protects mesenchymal stem cells from oxidative stress: a bioevaluation and mechanistic chemistry. *BMC Complement. Altern. Med.* **2016**, *16*, 423. [[CrossRef](#)] [[PubMed](#)]
36. Benzie, I.F.; Strain, J.J. The ferric reducing ability of plasma (FRAP) as a measure of “antioxidant power”: The FRAP assay. *Anal. Biochem.* **1996**, *239*, 70–76. [[CrossRef](#)] [[PubMed](#)]
37. Wang, T.T.; Zeng, G.C.; Li, X.C.; Zeng, H.P. In vitro studies on the antioxidant and protective effect of 2-substituted-8-hydroxyquinoline derivatives against H<sub>2</sub>O<sub>2</sub>-Induced oxidative stress in BMSCs. *Chem. Biol. Drug Des.* **2010**, *75*, 214–222. [[CrossRef](#)] [[PubMed](#)]
38. Wang, G.; Li, X.; Zeng, H. Synthesis, antioxidation activity of (E)-9-p-Tolyl-3-[2-(8-hydroxy-quinol-2-yl)vinyl]-carbazole and (E)-9-(p-Anisyl)-3-[2-(8-hydroxy-quinol-2-yl)vinyl]-carbazole and their induction proliferation of mesenchymal stem cells. *Acta Chim. Sin.* **2009**, *67*, 974–982.
39. Li, X.C.; Gao, Y.X.; Li, F.; Liang, A.F.; Xu, Z.M.; Bai, Y.; Mai, W.Q.; Han, L.; Chen, D.F. Maclurin protects against hydroxyl radical-induced damages to mesenchymal stem cells: Antioxidant evaluation and mechanistic insight. *Chem. Biol. Interact.* **2014**, *219*, 221–228. [[CrossRef](#)] [[PubMed](#)]
40. Li, X.C.; Han, L.; Li, Y.R.; Zhang, J.; Chen, J.; Lu, W.B.; Zhao, X.J.; Lai, Y.T.; Chen, D.F.; Wei, G. Protective effect of sinapine against hydroxyl radical-induced damage to mesenchymal stem cells and possible mechanisms. *Chem. Pharm. Bull.* **2016**, *64*, 319–325. [[CrossRef](#)] [[PubMed](#)]

41. Jiang, Q.; Li, X.C.; Tian, Y.G.; Lin, Q.; Xie, H.; Lu, W.B.; Chi, Y.G.; Chen, D.F. Lyophilized aqueous extracts of *Mori Fructus* and *Mori Ramulus* protect mesenchymal stem cells from  $\bullet\text{OH}$ -treated damage: Bioassay and antioxidant mechanism. *BMC Complement. Altern. Med.* **2017**, *17*, 242. [[CrossRef](#)] [[PubMed](#)]
42. Li, X.; Mai, W.; Chen, D.F. Chemical study on protective effect against hydroxyl-induced DNA damage and antioxidant mechanism of myricitrin. *J. Chin. Chem. Soc.* **2014**, *61*, 383–391. [[CrossRef](#)]
43. Li, X.; Wu, X.; Huang, L. Correlation between antioxidant activities and phenolic contents of radix *Angelicae sinensis* (Danggui). *Molecules* **2009**, *14*, 5349–5361. [[CrossRef](#)] [[PubMed](#)]
44. Tian, Y.; Li, X.; Xie, H.; Wang, X.; Xie, Y.; Chen, C.; Chen, D. Protective mechanism of the antioxidant baicalein toward hydroxyl radical-treated bone marrow-derived mesenchymal stem cells. *Molecules* **2018**, *23*, 223. [[CrossRef](#)]

**Sample Availability:** Samples of the compounds (+)-catechin and (–)-catechin gallate are available from the authors.



© 2018 by the authors. Licensee MDPI, Basel, Switzerland. This article is an open access article distributed under the terms and conditions of the Creative Commons Attribution (CC BY) license (<http://creativecommons.org/licenses/by/4.0/>).